JCTC Journal of Chemical Theory and Computation

ARTICLE

pubs.acs.org/JCTC

# Fully Relativistic Calculations of Faraday and Nuclear Spin-Induced Optical Rotation in Xenon

Suvi Ikäläinen,*[,†] Perttu Lantto,[‡] and Juha Vaara[‡]

[†]Laboratory of Physical Chemistry, Department of Chemistry, P.O. Box 55 (A.I. Virtasen aukio 1), FIN-00014 University of Helsinki, Finland

[‡]NMR Research Group, Department of Physics, P.O. Box 3000, FIN-90014 University of Oulu, Finland

Supporting Information

**ABSTRACT:** Nuclear spin-induced optical rotation (NSOR) arising from the Faraday effect may constitute an advantageous novel method for the detection of nuclear magnetization. We present first-principles nonrelativistic and relativistic, two- and four-component, basis-set limit calculations of this phenomenon for xenon. It is observed that only by utilization of relativistic methods may one qualitatively reproduce experimental liquid-state NSOR data. Relativistic effects lower the results by 50% as compared to nonrelativistic values. Indeed, relativistic Hartree−Fock calculations at the four-component or exact two-component (X2C) level account for the discrepancy between experimental results and earlier nonrelativistic theory. The nuclear magnetic shielding constant of traditional nuclear magnetic resonance as well as the Verdet constant parametrizing optical rotation due to an external magnetic field were also calculated. A comparison between results obtained using Hartree−Fock and density-functional theory methods at relativistic and nonrelativistic levels, as well as coupled cluster methods at the nonrelativistic level, was carried out. Completeness-optimized basis sets were employed throughout, for the first time in fully relativistic calculations. Full relativity decreases the Verdet constant by 4%. X2C theory decreases the absolute value of NSOR by 10−20% as compared to the four-component data, while for Verdet constants, the results are only slightly smaller than the fully relativistic values. For both properties, two-component calculations decrease the computational time by roughly 90%. Density-functional methods yield substantially larger values of NSOR than the Hartree−Fock theory or experiments. Intermolecular interactions are found to decrease NSOR and, hence, compensate for the electron correlation effect.

## 1. INTRODUCTION

Optical phenomena have been discussed in many recent studies[1−12] as novel methods for the detection of nuclear magnetic resonance (NMR). Optical effects may be more readily observed and carry the possibility of enhanced spatial resolution as compared to traditional radio frequency detection. These phenomena are based on the Faraday and inverse Faraday effects. In the Faraday effect, a magnetic field causes the plane of polarization of a linearly polarized (LPL) light beam, directed along the field, to rotate.[13] The field due to spin-polarized nuclei in an NMR sample accordingly also causes rotation in the plane of polarization of the incident LPL, in what is called the nuclear spin-induced optical rotation (NSOR).[9] Arising from the opposite phenomenon of the inverse Faraday effect, the laser-induced NMR shift has been investigated theoretically in refs 1−8, of which refs 6−8 report first-principles calculations of the magnitude of the phenomenon. It has been seen that, at least far away from the immediate vicinity of optical resonances, the effect is far too small to be measured. The NSOR has, however, been observed experimentally for protons in liquid water and liquid $^{129}$Xe in ref 9 and $^{19}$F in fluorocarbons in ref 12. First-principles nonrelativistic (NR) theoretical evaluation of NSOR has been carried out for ethanol, nitromethane, water, and urea in ref 11, where excellent agreement with experimental results was achieved for liquid water. Chemical distinction between different molecules and inequivalent nuclei in the same molecule has been predicted[11] and observed,[12] which implies that NSOR could provide a viable and potentially more informative analogue to the NMR chemical shift of traditional NMR detection. For ethanol, immense amplification of the effect was observed at laser frequencies close to optical resonances.[11] Enhanced chemical distinction between optically excited chromophores in the light-sensitive retinal model PSB-11 was also demonstrated.[11] A study regarding the intermolecular interaction effects on the NSOR due to $^{1}$H and $^{17}$O nuclei in $H_2O(l)$ has also been conducted recently,[14] demonstrating a close cancellation of the solvation and local optical field effects for $^{1}$HSOR.

The laser-induced shift and the NSOR are calculated through a similar third-order perturbational expression, essentially that of molecular antisymmetric polarizability,[1,2] and are easily interconverted.[9,11] In ref 9, the experimental results for liquid $^{129}$Xe were compared to NR theoretical values of the laser-induced shift obtained in ref 7. A qualitative agreement was observed, but it was subsequently realized that a factor of 2 had been neglected in the theory of ref 7, destroying the compatibility of the results. This implies that relativistic effects may be relevant for NSOR in $^{129}$Xe.

The importance of relativistic effects for accurate calculations of NSOR for heavy nuclei arises from the quantum mechanical

**Received:** September 12, 2011
**Published:** November 08, 2011

hyperfine operator that is involved in the antisymmetric polarizability, accountable for NSOR. In addition to the demands placed on the description of the electronic structure of the inner shells due to the hyperfine operator, the calculation of both NSOR and the Verdet constant (parametrizing the conventional Faraday rotation due to an external magnetic field) requires accurate electronic structure also at the outskirts of the electronic cloud, as this region is readily distorted by the external electric field, with significant contributions to the polarizability. Basis sets of high quality must therefore be used, which leads us to utilization of the completeness optimization[15] to generate basis sets designed specifically for the basis-set limit calculation of NSOR in $^{129}$Xe.

Here, we aim to demonstrate the importance and magnitude of relativistic effects on $^{129}$Xe NSOR in gaseous and liquid xenon through fully relativistic (strictly true only for the one-particle part of the molecular Hamiltonian[16]) four-component Dirac–Fock (DHF) and Dirac–DFT (DDFT) calculations. $^{129}$XeSOR has been calculated at standard visible or near-infrared laser frequencies. We have also evaluated the Verdet constant for xenon as well as, to further evaluate the basis set used, the nuclear shielding constant of traditional NMR. The DHF results are compared to relativistic, sc. exact two-component (X2C)[17] data as well as NR HF results. Relativistic and NR calculations were carried out at the HF and density functional theory (DFT) levels, and both the collinear and the noncollinear spin density definitions were used in the relativistic code for the latter. NR coupled cluster singles and doubles (CCSD) values were computed to calibrate the performance of the DFT functionals. Novel and compact completeness-optimized basis sets, which have been shown to produce results close to the basis-set limit for magnetic properties,[8,11,15,18] were employed here in a first application to fully relativistic calculations. Basis-set convergence for the nuclear shielding constant in atomic $^{129}$Xe is also of present interest, as it earlier turned out to be demanding by a Gaussian basis-set expression[19−21] to approach the numerical limiting value.[22]

## 2. THEORY

**2.1. Nuclear Spin-Induced Optical Rotation.** The magnetic optical rotation angle $\Phi$ per unit of sample length $l$ can be written as[23−25]

$$\frac{\Phi}{l} = \frac{1}{2}\omega\mathcal{N}\mu_0 c\mathrm{Im}\langle\alpha'_{XY}\rangle \tag{1}$$

where $\omega$ is the frequency of the laser beam propagating in the laboratory $Z$ direction, $\mathcal{N}$ is the number density, $c$ denotes the speed of light *in vacuo*, and $\langle\boldsymbol{\alpha}'\rangle$ is the ensemble-averaged, complex antisymmetric polarizability. For an external magnetic field $\mathbf{B}_0$ and nuclear spin component $I_{K,Z}$ along the beam[1,10]

$$\alpha'_{XY} = \alpha'^{(B_0)}_{XY,Z}B_0 + \alpha'^{(I_K)}_{XY,Z}I_{K,Z} + \mathcal{O}(B_0^3, I_K^3) \tag{2}$$

Molecular tumbling in gaseous or liquid samples leads to the isotropic molecular average

$$\langle\alpha'_{XY,Z}\rangle = \frac{1}{6}\sum_{\varepsilon\tau\nu}\varepsilon_{\varepsilon\tau\nu}\alpha'_{\varepsilon\tau,\nu} = \frac{1}{3}(\alpha'_{xy,z} + \alpha'_{yz,x} + \alpha'_{zx,y}) \tag{3}$$

where $\varepsilon_{\varepsilon\tau\nu}$ is the Levi–Civita symbol and $(x,y,z)$ are coordinates in the molecule-fixed Cartesian frame. For an atom, the three components are equal and $\langle\alpha'_{XY,Z}\rangle = \alpha'_{xy,z}$. $\alpha'^{(B_0/I_K)}_{\varepsilon\tau,\nu}$ may be calculated through a third-order perturbation theoretical equation[1,2] that, in the notation of quadratic response theory,[6,26] is written as

$$\alpha'^{(B_0/I_K)}_{\varepsilon\tau,\nu} = -\langle\langle\mu_\varepsilon;\mu_\tau,h_\nu^{Z/\mathrm{hf}}\rangle\rangle_{\omega,0} \tag{4}$$

with $\mu_\varepsilon$ and $\mu_\tau$ arising from the components of the dipole moment. In eq 4, the expression of conventional electric dipole polarizability, $\boldsymbol{\alpha}(\omega) = -\langle\langle\boldsymbol{\mu};\boldsymbol{\mu}\rangle\rangle_\omega$, is modified by a third, static magnetic operator $h$. For optical rotation caused by an external field $\mathbf{B}_0$, this operator is the Zeeman interaction, whereas for NSOR, $h$ is the hyperfine interaction. The relativistic perturbation operators are defined through

$$H_Z = \sum_\nu h_\nu^Z B_{0,\nu}; \quad H_{hf} = \sum_K\sum_\nu h^{\mathrm{hf}}_{K,\nu}I_{K,\nu} \tag{5}$$

for the Zeeman and hyperfine interactions, respectively, where

$$h_\nu^Z = -\frac{ce}{2}\sum_{i=1}^{N_{el}}(\boldsymbol{\alpha}\times\mathbf{r}_{iO})_\nu \tag{6}$$

and

$$h^{\mathrm{hf}}_{K,\nu} = -\frac{ce\mu_0\hbar}{4\pi}\sum_{i=1}^{N_{el}}\frac{\gamma_K(\boldsymbol{\alpha}\times\mathbf{r}_{iK})_\nu}{r_{iK}^3} \tag{7}$$

Here, $\boldsymbol{\alpha}$ is the Dirac $4\times4$ matrix operator, $N_{el}$ is the number of electrons, $\gamma_K$ is the gyromagnetic ratio of nucleus $K$, and $\mathbf{r}_{iK}$ the vector from the nucleus $K$. In one-component NR theory, the familiar orbital Zeeman (OZ) and paramagnetic nuclear spin-electron orbit (PSO) operators[11] replace the operators of eqs 6 and 7, respectively.

In the case of optical rotation caused by an external field $\mathbf{B}_0$, $\Phi = VB_0l$, where the Verdet constant $V$ is

$$V = -\frac{1}{2}\omega\mathcal{N}\mu_0 ce^2\frac{1}{6}\sum_{\varepsilon\tau\nu}\varepsilon_{\varepsilon\tau\nu}\mathrm{Im}\langle\langle r_\varepsilon;r_\tau,h_\nu^Z\rangle\rangle_{\omega,0} \tag{8}$$

For optical rotation arising from nuclear spins, for unit concentration $[] = \mathcal{N}/N_A$ of the polarized nuclei $K$,

$$\frac{\Phi_{\mathrm{NSOR}}}{[]l} = -\frac{1}{2}\omega N_A\mu_0 ce^2\langle I_{K,Z}\rangle\frac{1}{6}\sum_{\varepsilon\tau\nu}\varepsilon_{\varepsilon\tau\nu}\mathrm{Im}\langle\langle r_\varepsilon;r_\tau,h^{\mathrm{hf}}_{K,\nu}\rangle\rangle_{\omega,0} \tag{9}$$

where $\langle I_{K,Z}\rangle$ is the average spin polarization.

The NSOR and the laser-induced shift, $\Delta$, can be related through the equation

$$\frac{\Phi_{\mathrm{NSOR}}}{[]l} = -h\omega N_A\langle I_{K,Z}\rangle\frac{\Delta}{I_0} \tag{10}$$

where $I_0$ is the intensity of the incident, circularly polarized beam in the inverse Faraday effect.

**2.2. Completeness-Optimized Basis Sets.** The concept of completeness optimization was first introduced by Manninen and Vaara in ref 15 as a novel method of generating high-quality Gaussian basis sets with relatively few functions. In the completeness-optimization scheme, energetic criteria for basis-set generation are discarded allowing, in principle, creation of universal (element-independent) basis sets that are systematically and economically extended for basis-set limit calculations of a specific property. Completeness profiles presented by Chong[27] are employed. The completeness profile is defined as

$$Y(\zeta) = \sum_m\langle g(\zeta)|\chi_m\rangle^2 \tag{11}$$

where $\{\chi\}$ is a set of orthonormalized basis functions for a given angular momentum $l$ and $g(\zeta)$ is an arbitrary "test" Gaussian $l$-type orbital (GTO) with the exponent $\zeta$. $g(\zeta)$ is used to analyze the completeness of $\{\chi\}$, and for a complete set, the value of $Y(\zeta)$ is equal to 1 for all $\zeta$. $Y(\zeta)$ can be portrayed on a $[\log(\zeta),Y(\zeta)]$ plot, in which case the profile of a basis set that is complete for a certain range of $\zeta$ will create a plateau-like figure, an example of which may be seen in the Supporting Information, where the completeness profile for the basis set used presently is displayed. Completeness-optimized basis sets are generated using the Kruununhaka code,[28] in which one may specify the desired exponent range $[\zeta_{min},\zeta_{max}]$ and the number of GTOs. The code will then generate a primitive basis set using these criteria, for which the measure of the deviation from completeness[15]

$$\tau = \int_{\zeta_{min}}^{\zeta_{max}} [1 - Y(\zeta)]\, d\zeta \qquad (12)$$

will be as small as possible, resulting in a compact basis set that will typically produce more accurate results for magnetic properties than traditional energy-optimized basis sets of the same size.[8,15,18]

## 3. CALCULATIONS

Completeness optimization was used to generate the large-component (LC) basis sets. The small-component (SC) basis sets used in the relativistic calculations were obtained via restricted kinetic balance (RKB) or unrestricted kinetic balance (URKB).[16] The basis sets were obtained by first generating a set that, for the different $l$ values, spans the same exponent ranges as in the cv4z basis of Dyall,[29] maintaining the deviation $\tau$ from completeness [eq 12] under 0.001. The exponent ranges were then systematically extended by tight and diffuse exponents, for each $l$ value separately, using a sufficient number of Gaussian functions to span the desired area to high accuracy. Trial DHF calculations of $^{129}$Xe nuclear shielding and $^{129}$XeSOR were conducted, and an exponent range that no longer significantly changed the results was chosen as a reference. The number of exponents was then reduced for each of the $l$ values separately, and the basis set giving results for the nuclear shielding constant and NSOR deviating by under 0.5 ppm and 1%, respectively, from the reference values, was chosen as the "co" basis set with the final composition (35s32p24d3f). The exponents and completeness profile of this basis set are available in the Supporting Information.

All relativistic calculations of $\Phi_{NSOR}$, $V$, and the nuclear shielding constant $\sigma$ were conducted with the Dirac[30] program, while all NR calculations were carried out with the Dalton program.[31] Verdet constants are reported for both gaseous and liquid Xe. The gas number density $\mathcal{N}$ required for the conversion of the calculated single-atom response functions to real gas situation was obtained through the van der Waals equation for real xenon gas,[32] which yields $\mathcal{N} = 2.58\times 10^{25}$ m$^{-3}$ at STP. Calculations were done at standard UV/NIR laser frequencies using HF and different DFT methods as well as NR CCSD. The DFT functionals BLYP,[33,34] B3LYP,[34−36] and BHandHLYP,[34,37] with increasing amounts of the exact HF exchange (0%, 20%, and 50%, respectively) were employed. The four-component relativistic calculations of nuclear shielding were carried out using full linear response theory, i.e., without replacing the *ep* branch of the response function with the corresponding NR diamagnetic operator, as is sometimes done in four-component theory.[19,38] In addition to four-component calculations, two-component (X2C)[17] results were also computed for $\Phi_{NSOR}$ and $V$. X2C values are not reported for the nuclear shielding constant, as the diamagnetic part of the shielding is not yet properly accounted for in the X2C scheme of the Dirac program. Quadratic response functions were used for HF, DFT, and CCSD, the implementations of which are covered in refs 39, 40, and 41, respectively, for the Dalton program, and refs 42 and 43 for the Dirac code.

The basis-set convergence of Dyall's vxz and cvxz[29,44,45] basis set families was investigated for $\Phi_{NSOR}$, $V$, and $\sigma$ with the HF method. The effects of using either RKB or URKB for the generation of the SC basis sets was also investigated. The completeness-optimized basis set was then used for calculations of all of the discussed properties with the DHF, X2C (omitting $\sigma$), and NR HF methods to determine relativistic effects. The co basis set was also used at the different DFT levels (at the four-component and NR levels), for which relativistic calculations using both the non-collinear[46] and collinear definitions of the spin density were also performed. All calculations involving the co basis were carried out with URKB.

The effects of numerical approximations as well as the inclusion and exclusion of two-electron integral classes were tested comprehensively, but results are not given here, as the deviation between the results was minimal. The convergence thresholds for the wave function and the response functions were dropped by a factor of 10 from the Dirac defaults in separate calculations. A convergence threshold of $1.2\times 10^{-5}$ was used for the wave function optimization, while $1.0\times 10^{-7}$ was used for both linear and quadratic response functions. A calculation using the full set on two-electron integrals as well as calculations excluding the small−small (SS) integrals from the response, excluding both the SS and large−small (LS) integrals from the response, as well as a calculation excluding the SS integrals from both the response and wave function optimization, were also conducted. The reported results are obtained via excluding SS integrals in the response as well as SCF. The same approximation was found to be entirely adequate for Verdet constants in ref 47.

## 4. RESULTS AND DISCUSSION

**4.1. Basis-Set Convergence with Standard Sets.** The basis set convergence of the NSOR angle and the Verdet constant at 514.5 nm, as well as the nuclear shielding constant as a function of the number of basis functions (LC functions for relativistic results) of the Dyall basis set families is shown in Figure 1. The DHF URKB results given by the co basis set are also displayed. Tables S2−S4 in the Supporting Information list $\Phi_{NSOR}/([]l)$ and $V$ at the different laser wavelengths, along with $\sigma$, using the Dyall basis set families and same levels of theory as in Figure 1. RKB results are omitted from the tables for NSOR and $V$, as they are identical to the URKB values to the displayed accuracy. Table 1 gives the number of basis functions (LC and SC) for the Dyall and co basis sets.

As in previous studies,[9,11] it is seen that the magnitude of $\Phi_{NSOR}/([]l)$ decreases as the laser wavelength increases. The difference between RKB and URKB data is practically negligible for NSOR, and dyall.vxz and dyall.cvxz results are very close to each other, although the addition of tight functions in the cvxz series increases NSOR slightly. The inclusion of relativity decreases absolute values of $\Phi_{NSOR}/([]l)$ by roughly 15−30%. It is seen that the results with the two Dyall basis set series are not converged as a function of the basis set size. Furthermore, they are monotonically increasing, away from the basis-set limit value obtained with the presently developed co basis set. Indeed,

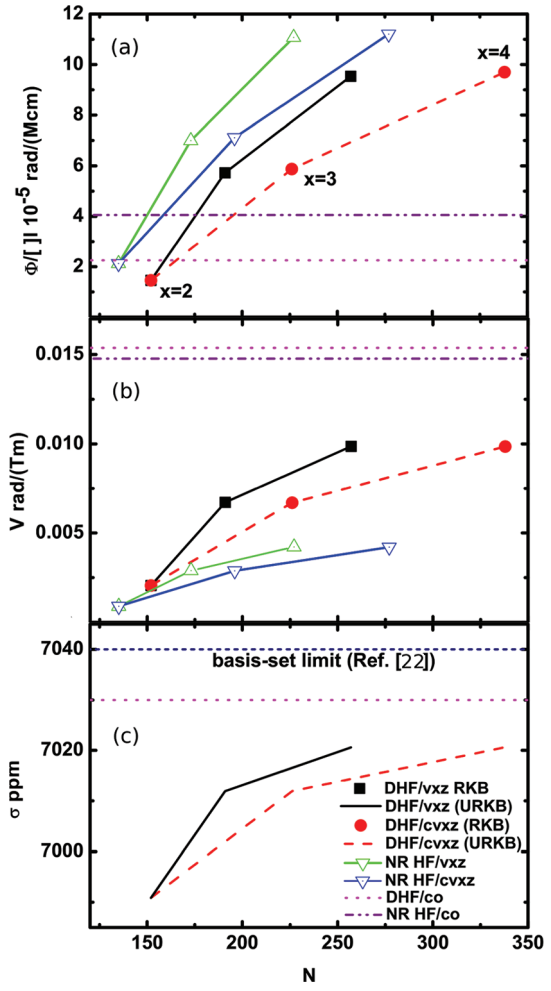


**Figure 1.** (a) $^{129}$Xe nuclear spin optical rotation angle $\Phi_{NSOR}/([]l)$ [in $10^{-5}$ rad/(M cm)], (b) the Verdet constant $V$ [in rad/(T m)] (both properties at 514.5 nm), as well as (c) the nuclear shielding constant $\sigma$ [in ppm] for gaseous Xe as a function of the number of basis functions $N$ using the Dyall vxz and cvxz basis sets and the nonrelativistic (NR) as well as relativistic (DHF) Hartree−Fock method. Both the restricted and unrestricted kinetic balance (RKB and URKB, respectively) were used for the latter. The results obtained with the co basis set (with $N = 305$) are shown as horizontal lines. Due to the large offset in results, the NR and DHF/RKB data for $\sigma$ are not shown.

**Table 1. Number of Large-Component (LC) and Small-Component (SC) Basis Functions in the Dyall and co Basis Sets**

| | | SC | | total | |
|---|---|---|---|---|---|
| basis set | LC | RKB | URKB | RKB | URKB |
| dyall.v2z | 152 | 177 | 353 | 329 | 505 |
| dyall.v3z | 191 | 224 | 447 | 415 | 638 |
| dyall.v4z | 257 | 298 | 595 | 555 | 852 |
| dyall.cv3z | 226 | 260 | 520 | 486 | 746 |
| dyall.cv4z | 338 | 382 | 763 | 720 | 1101 |
| co | 305 | | 704 | | 1009 |

augmentation of the dyall.v4z basis with diffuse $d$-type functions (obtained by successively dividing the most diffuse exponent by 3)

**Table 2. $^{129}$Xe Nuclear Spin Optical Rotation $\Phi_{NSOR}/([]l)$ [in $10^{-5}$ rad/(M cm)] for Different Laser Wavelengths at the Hartree−Fock Level Using the Completeness-Optimized Basis Set co and the Fully Relativistic Four-Component (DHF), Exact Two-Component (X2C), and Nonrelativistic (NR) Methods (Experimental Results Are Also Given)**

| $\lambda$ (nm) | $\omega$ (au) | NR | X2C | DHF | \|exptl.\|[a] |
|---|---|---|---|---|---|
| 488.8 | 0.0932147 | −4.65 | −2.30 | −2.63 | |
| 514.5 | 0.0885585 | −4.05 | −1.97 | −2.25 | |
| 532.0 | 0.0856454 | −3.71 | −1.78 | −2.04 | 1.5 ± 0.3 |
| 589.0 | 0.0773571 | −2.87 | −1.32 | −1.53 | |
| 694.3 | 0.0656249 | −1.92 | −0.84 | −0.99 | |
| 770.0 | 0.0591732 | −1.51 | −0.64 | −0.76 | 0.6 ± 0.1 |
| 1064.0 | 0.0428227 | −0.74 | −0.29 | −0.35 | 0.4 ± 0.2 |
| 1319.0 | 0.0345439 | −0.47 | −0.18 | −0.22 | |

[a] Liquid-state experimental results from ref 9.

**Table 3. Verdet Constant $V$ [in $10^{-3}$ rad/(T m)] for Gaseous Xe at Different Laser Wavelengths Using the Completeness-Optimized Basis Set co and the Fully Relativistic Four-Component (DHF), Exact Two-Component (X2C), and Nonrelativistic (NR) Hartree−Fock Methods (Previous Relativistic Computational and Experimental Results Are Also Given)**

| $\lambda$ (nm) | $\omega$ (au) | NR | X2C | DHF | ref 47[a] | \|exptl.\|[b] |
|---|---|---|---|---|---|---|
| 488.8 | 0.0932147 | 16.53 | 17.31 | 17.23 | | |
| 514.5 | 0.0885585 | 14.77 | 15.44 | 15.37 | 15.59 | |
| 532.0 | 0.0856454 | 13.73 | 14.35 | 14.28 | | |
| 589.0 | 0.0773571 | 11.02 | 11.49 | 11.44 | | 12.30 |
| 694.3 | 0.0656249 | 7.77 | 8.09 | 8.06 | 8.15 | |
| 770.0 | 0.0591732 | 6.26 | 6.51 | 6.48 | | |
| 1064.0 | 0.0428227 | 3.21 | 3.34 | 3.32 | 3.37 | |
| 1319.0 | 0.0345439 | 2.08 | 2.15 | 2.15 | | |

[a] DHF results using the well tempered-basis set by Huzinaga augmented with diffuse functions. Values in the table have been converted to real gas number density. Original values obtained in ref 47 are 55.16, 28.85, and 11.91 $\mu$min/(G cm) at $\omega$ = 0.088599, 0.065600, and 0.042823 au, respectively, for an ideal gas. [b] Experimental result from ref 48.

alters the results (not shown) dramatically toward the co values. As before,[8,11] the antisymmetric polarizability responsible for NSOR is very challenging even for high-quality basis sets designed for studying standard chemical problems.

Similarly to NSOR, the magnitude of $V$ increases with frequency, and RKB and URKB data are in practice equivalent. Additional functions in the dyall.cvzx sets do not particularly affect the results, which is expected, as no hyperfine operators are involved. For the same reason, the NR results are only 3−5% lower than the relativistic results, as the response of the valence-only operators of $V$ is less sensitive to changes in the description of the atomic core region than in the case of NSOR. As in earlier work,[47] the Verdet constants are underestimated by basis sets that lack sufficiently diffuse functions.

From Table S4 (Supporting Information), it is seen that for $\sigma$, the use of URKB clearly improves the results and is therefore necessary to approach the basis-set limit with sets of the size of the Dyall basis set families. In the URKB case, the more complete small-component basis set is important for the part of $\sigma$

corresponding to negative-energy excited states. In calculations with URKB, the magnitude of $\sigma$ increases by 400−500 ppm as compared to RKB results, and the series starts to show signs of convergence. The NR data are approximately 1400 ppm lower than the relativistic URKB data. In contrast to the case of NSOR, additional diffuse *d* functions on top of the Dyall v4z basis do not affect $\sigma$. The best results with the Dyall basis sets are approximately 10 ppm lower than the co result and 20 ppm below the basis-set limit of 7040 ppm.[22]

**4.2. Four-Component, Two-Component, and NR Calculations.** We turn to nearly basis-set limit calculations using our present co basis set. Tables 2 and 3 display NSOR and the Verdet constant as functions of the laser wavelength at the fully relativistic four-component DHF, two-component X2C, and NR HF levels, with the co basis set. The corresponding nuclear shielding data are included in Table S4 (Supporting Information). Experimental results are also reported for NSOR and *V*. Figure 2 illustrates $|\Phi_{NSOR}/([]l)|$ and *V*, the latter for gaseous Xe. Going from the NR calculations to full relativity decreases the absolute value of $^{129}$XeSOR by roughly 40−50%. DHF results are in reasonably good agreement with the experimental values taking the error limits of the latter into account. Table 2 shows that the good correspondence between the NR calculations of ref 7 with experimental results discussed in ref 9 was indeed due to the absence of a factor of 2 in the analysis of ref 7. The present inclusion of relativity brings the results back close to the experimental values. The X2C method further reduces NSOR as compared to DHF, producing (fortuitously) a still slightly improved agreement with experimental results.

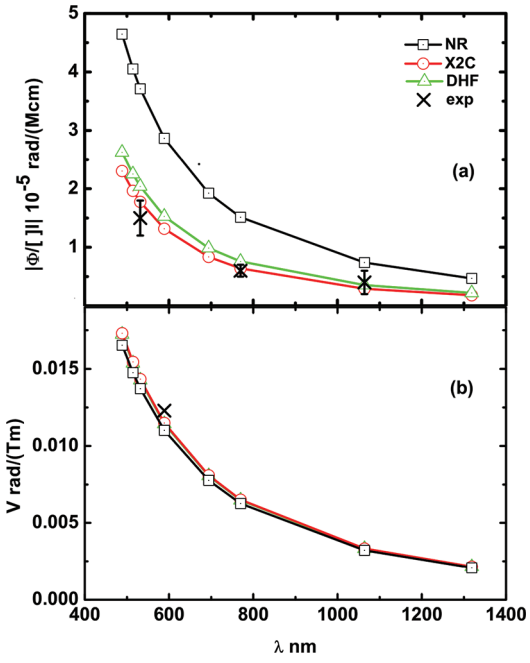


**Figure 2.** (a) $^{129}$Xe nuclear spin optical rotation $|\Phi_{NSOR}/([]l)|$ [in $10^{-5}$ rad/(M cm)] and (b) Verdet constant *V* rad/(T m)] for gaseous Xe at different laser wavelengths using the completeness-optimized basis set co and the fully relativistic four-component (DHF), exact two-component (X2C), and nonrelativistic (NR) Hartree−Fock methods. The experimental data from refs 9 and 48 are also shown.

For the Verdet constant, the NR results are below the DHF data by ∼4%, whereas the X2C calculations yield slightly larger values still. The DHF and X2C results are close to the experimental[48] value at $\lambda$ = 589.0 nm as well as the previous computational DHF results[47] obtained with an augmented well-tempered Huzinaga basis set.

**4.3. Correlation Effects with the DFT Method.** Table 4 and Tables S5 and S6 in the Supporting Information give NSOR, *V*, and $\sigma$ at HF and various DFT levels of theory, for both noncollinear and collinear treatment of the spin density in the case of DDFT. NR CCSD results are also displayed. Figure 3 illustrates NSOR and the Verdet constant as a function of wavelength with the HF and DFT methods. For all properties, it is seen that the collinear and noncollinear approaches give nearly identical results, and the numerical values indicate that the small difference further diminishes with increasing exact exchange admixture in the DFT functional in the series from BLYP via B3LYP to BHandHLYP. The increase in the amount of exact exchange leads to an overall decrease in $|\Phi_{NSOR}|$ toward the HF values. The DFT results remain significantly larger than the HF results, by ∼50−100% and 70−300% at the NR and four-component levels, respectively. A smaller variation between the HF and DFT results is observed for *V*, for which DFT leads to increases of ∼10−40% and ∼15−50% at NR and relativistic levels. The DFT data are typically also in a much greater disagreement with experimental results than the HF results, with the exception of *V* at the BHandHLYP level, which is already rather close to the experimental result. Compared to NR HF, electron correlation at the NR CCSD level increases $^{129}$XeSOR by ∼65−75%, whereas a smaller relative

**Table 4. $^{129}$Xe Nuclear spin-induced optical rotation $\Phi_{NSOR}/([\,]\,l)$ [in $10^{-5}$ rad/(M cm)] at different laser wavelengths using the completeness-optimized basis set co with nonrelativistic (NR) as well as relativistic (Rel.) HF and different DFT methods. Both the non-collinear (NC) and collinear (C) spin density approaches were used for relativistic DFT. The nonrelativistic coupled-cluster singles and doubles (CCSD) results are also given.**

| | | DFT/BLYP | | | DFT/B3LYP | | | DFT/BHandHLYP | | | HF | | |
|---|---|---|---|---|---|---|---|---|---|---|---|---|---|
| $\gamma$ (nm) | $\omega$ (a.u.) | NR | Rel. C | Rel. NC | NR | Rel. C | Rel. NC | NR | Rel. C | Rel. NC | NR | Rel. | NR CCSD |
| 488.8 | 0.0932147 | −14.60 | −11.32 | −11.24 | −10.70 | −7.73 | −7.68 | −7.18 | −4.54 | −4.54 | −4.65 | −2.63 | −7.65 |
| 514.5 | 0.0885585 | −12.77 | −9.86 | −9.79 | −9.36 | −6.73 | −6.68 | −6.28 | −3.93 | −3.93 | −4.05 | −2.25 | −6.71 |
| 532.0 | 0.0856454 | −11.71 | −9.03 | −8.96 | −8.59 | −6.16 | −6.12 | −5.76 | −3.59 | −3.59 | −3.71 | −2.04 | −6.17 |
| 589.0 | 0.0773571 | −9.09 | −6.96 | −6.91 | −6.67 | −4.74 | −4.71 | −4.47 | −2.74 | −2.74 | −2.87 | −1.53 | −4.82 |
| 694.3 | 0.06562496 | −6.15 | −4.67 | −4.64 | −4.52 | −3.17 | −3.15 | −3.02 | −1.82 | −1.82 | −1.92 | −0.99 | −3.28 |
| 770.0 | 0.0591732 | −4.85 | −3.67 | −3.64 | −3.57 | −2.49 | −2.48 | −2.39 | −1.42 | −1.42 | −1.51 | −0.76 | −2.60 |
| 1064.0 | 0.0428227 | −2.39 | −1.79 | −1.78 | −1.76 | −1.21 | −1.21 | −1.17 | −0.68 | −0.68 | −0.74 | −0.35 | −1.29 |
| 1319.0 | 0.0345439 | −1.52 | −1.14 | −1.13 | −1.12 | −0.77 | −0.76 | −0.75 | −0.43 | −0.43 | −0.47 | −0.22 | −0.82 |


dx.doi.org/10.1021/ct200636m |J. Chem. Theory Comput. 2012, 8, 91–98

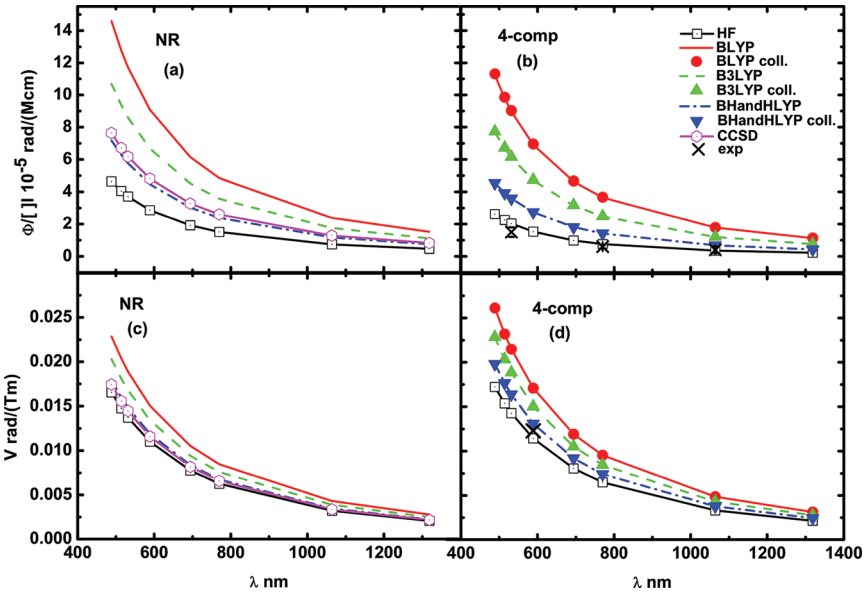


**Figure 3.** (a,b) $^{129}$Xe nuclear spin-induced optical rotation angle [in $10^{-5}$ rad/(M cm)] and (c,d) the Verdet constant [in rad/(T m)] for gaseous Xe at different laser wavelengths using the completeness-optimized basis set co and the Hartree−Fock (HF) method as well as density functional theory with BLYP, B3LYP, and BHandHLYP functionals. Nonrelativistic results are displayed on the left (a and c), while the relativistic results are given on the right (b and d).

increase of 5% is observed for $V$. For both properties at the NR level, BHandHLYP is closest to CCSD results. From the similar behavior of NR DFT and DDFT, and from the increase in NR $|\Phi_{NSOR}|$ in Figure 3 upon introduction of electron correlation, it can be conjectured that electron correlation would also increase the absolute values of $^{129}$XeSOR at the relativistic level, taking them further away from the experimental values. We presently lack the computational tools for correlated *ab initio* magnetic properties at the fully relativistic level. For $\sigma$, the HF and DFT values are very similar to each other.

**4.4. Comparison with Experimental Results.** It was seen in Figure 2 that inclusion of relativity brings the HF results for NSOR close to experimental values. However, it is also evident from Table 4 that electron correlation, also at the relativistic level (as estimated using DDFT), again renders these results further from the experimental ones. It seems as though our results for $^{129}$XeSOR based on isolated-atom calculations remain higher than the experimental values. The latter were obtained in liquid Xe, and the concentration of the atoms provides the connection of optical rotation, a bulk property, to the calculated antisymmetric polarizability of a single atom. Atomic and molecular properties change, however, when they are introduced to a medium. It was found in ref 14 that, for $^{1}$H in water, $\Phi_{NSOR}$ for an interacting molecule in the liquid phase is 14% smaller than NSOR for a static molecule *in vacuo*. For the oxygen nucleus, the NSOR is 29% smaller for interacting molecules. It is thus likely that $^{129}$XeSOR for liquid-phase Xe would also be lower than our *in vacuo* results. This was tested by performing a DHF calculation on a $^{129}$Xe dimer at its equilibrium geometry [$r_{Xe-Xe}$ = 4.3627 Å (ref 49)] with the co basis set, the results of which are reported in Table S7 of the Supporting Information. Although the co basis is not entirely converged for the interaction effect, it can be seen that the values of NSOR are indeed lowered by ∼35−45%. Hence, interatomic interactions are important for $^{129}$XeSOR, and their proper inclusion is likely to significantly improve the agreement with experimental optical rotation in a liquid medium.

## 5. CONCLUSIONS

Fully relativistic calculations of the nuclear spin-induced optical rotation at standard vis−near-IR laser frequencies were conducted for $^{129}$Xe, along with computations of the Verdet constant and nuclear shielding. Completeness optimization, a novel method for generation of basis sets that have been proven to be successful in calculations of magnetic properties, was used for the first time in fully relativistic calculations. The presently generated co basis set was compared to the Dyall basis set families, for which calculations were performed using both restricted and unrestricted kinetic balance. The significance of relativity was evaluated with calculations at fully relativistic four-component Dirac Hartree−Fock, exact two-component HF, and nonrelativistic HF levels of theory. Various DFT functionals were also utilized at NR and relativistic levels, for which both the collinear and noncollinear spin density approaches were examined. At the NR level, the ab initio CCSD method was used as a benchmark for electron correlation effects.

It was observed that the Dyall basis sets appear to converge to an erroneous basis-set limit for the present, very demanding property of NSOR. RKB and URKB give very similar results for both NSOR and Verdet constants. DHF and X2C results are relatively similar for $\Phi_{NSOR}$ and $V$. The relativistic and nonrelativistic HF Verdet constants are close to each other, with relativity adding a few percent to the results, similarly to earlier observations.[47] The results are close to experimental and previous DHF data. For $^{129}$XeSOR, full relativity lowers the NR results by 40−50%, while the X2C results remain still somewhat lower than DHF values. The inclusion of relativity is mandatory in order to reach a qualitative agreement with recent $^{129}$XeSOR experiments on liquid xenon. Earlier NR calculations by one of the present authors were fortuitously successful due to a missing numerical factor in the analysis.

All of the investigated DFT levels give larger values than HF of $^{129}$XeSOR and the Verdet constants in both relativistic and NR

calculations. Electron correlation effects estimated via NR CCSD calculations increase $^{129}$XeSOR and $V$ by ca. 70% and 5%, respectively. Among DFT results, BHandHLYP values are closest to experimental ones and, at the NR level, CCSD values, as noted before.[8] It can be concluded that while the uncorrelated DHF values for NSOR are closer to experimental results than DDFT data, the inclusion of electron correlation does lead to overestimation. These calculations were made for a noninteracting Xe atom, which led us to approximate the intermolecular interaction effects by performing a calculation for a Xe dimer. The results indicate that calculations involving interacting molecules would, in turn, decrease NSOR as compared to isolated molecules, bringing the values back closer to experimental ones. Hence, relativistic, electron correlation, and intermolecular interaction effects are all important for heavy-atom NSOR.

## ■ ASSOCIATED CONTENT

**Supporting Information.** Exponents and the completeness profile of the co basis set; tables of NSOR and Verdet constants (for gaseous $^{129}$Xe) at different wavelengths, as well as nuclear shielding using the Dyall basis set families (nonrelativistic and four-component Hartree−Fock methods); tables of NSOR, Verdet constants (for gaseous $^{129}$Xe) at different wavelengths, and nuclear shielding using the co basis set at the Hartree−Fock and different DFT levels using nonrelativistic and four-component theory, for which noncollinear and collinear definitions of spin density were used for all of the DFT functionals; table of NSOR for the interacting Xe dimer and noninteracting atom at different wavelengths at the co/DHF level. This material is available free of charge via the Internet at http://pubs.acs.org/.

## ■ AUTHOR INFORMATION

### Corresponding Author

*E-mail: suvi.ikalainen@helsinki.fi.

### Notes

The authors declare no competing financial interest.

## ■ ACKNOWLEDGMENT

We thank Prof. Michael V. Romalis (Princeton) for useful discussions. The authors belong to the Finnish CoE in Computational Molecular Science. Support was received from the Graduate School of Computational Chemistry and Molecular Spectroscopy (S.I.), the Alfred Kordelin Fund (S.I.), Academy of Finland (P.L., J.V.), and U. Oulu (J.V.). Computational resources due to CSC (Espoo, Finland) were used. P.L. is an academy research fellow of the Academy of Finland.

## ■ REFERENCES

(1) Buckingham, A. D.; Parlett, L. C. *Science* **1994**, *264*, 1748.
(2) Buckingham, A. D.; Parlett, L. C. *Mol. Phys.* **1997**, *91*, 805.
(3) Warren, W. S.; Mayr, S.; Goswamy, D.; West, A. P., Jr. *Science* **1992**, *255*, 1683.
(4) Harris, R. A.; Tinoco, I., Jr. *J. Chem. Phys.* **1994**, *101*, 9289.
(5) Li, L.; He, T.; Chen, D.; Wang, X.; Liu, F.-C. *J. Phys. Chem.* **1998**, *102*, 10385.
(6) Jaszuński, M.; Rizzo, A. *Mol. Phys.* **1999**, *96*, 855.
(7) Romero, R. H.; Vaara, J. *Chem. Phys. Lett.* **2004**, *400*, 226.
(8) Ikäläinen, S.; Lantto, P.; Manninen, P.; Vaara, J. *J. Chem. Phys.* **2008**, *129*, 124102.
(9) Savukov, I. M.; Lee, S. K.; Romalis, M. V. *Nature (London)* **2006**, *442*, 1021.
(10) Lu, T.; He, M.; Chen, D.; He, T.; Liu, F.-C. *Chem. Phys. Lett.* **2009**, *479*, 14.
(11) Ikäläinen, S.; Romalis, M. V.; Lantto, P.; Vaara, J. *Phys. Rev. Lett.* **2010**, *105*, 153001.
(12) Pagliero, D.; Dong, W.; Sakellariou, D.; Meriles, C. A. *J. Chem. Phys.* **2010**, *133*, 154505.
(13) Barron, L. D. *Molecular Light Scattering and Optical Activity*, 2nd ed.; Cambridge University Press: Cambridge, U.K., 2004; pp 145−147.
(14) Pennanen, T. S.; Ikäläinen, S.; Lantto, P.; Vaara, J. Submitted for publication.
(15) Manninen, P.; Vaara, J. *J. Comput. Chem.* **2006**, *27*, 434.
(16) Dyall, K. G.; Fægri, K., Jr. *Introduction to Relativistic Quantum Chemistry*; Oxford University Press: New York, 2007; p 200.
(17) Iliaš, M.; Saue, T. *J. Chem. Phys.* **2007**, *126*, 064102.
(18) Ikäläinen, S.; Lantto, P.; Manninen, P.; Vaara, J. *Phys. Chem. Chem. Phys.* **2009**, *11*, 11404.
(19) Vaara, J.; Pyykkö, P. *J. Chem. Phys.* **2003**, *118*, 2973.
(20) Saue, T. *Adv. Quantum Chem.* **2005**, *48*, 383.
(21) Hanni, M.; Lantto, P.; Iliaš, M.; Jensen, H. J. Aa.; Vaara, J. *J. Chem. Phys.* **2007**, *127*, 164313.
(22) Kolb, D.; Johnson, W. R.; Shorer, P. *Phys. Rev. A* **1982**, *26*, 19.
(23) Buckingham, A. D.; Stephens, P. J. *Annu. Rev. Phys. Chem.* **1966**, *17*, 399.
(24) Buckingham, A. D. *Phil. Trans. R. Soc. London, Ser. A* **1979**, *293*, 239.
(25) We use SI units throughout the paper. The positive $\Phi$ in eq 1 corresponds to a right-handed optical rotation as seen from the source.
(26) Olsen, J.; Jørgensen, P. *J. Chem. Phys.* **1985**, *82*, 3235.
(27) Chong, D. P. *Can. J. Chem.* **1995**, *73*, 79.
(28) Kruununhaka basis set tool kit, written by Manninen, P.; Lehtola, J. Release 2.0 (2011). http://www.chem.helsinki.fi/~manninen/kruununhaka/ (accessed February, 2011).
(29) Dyall, K. G. *Theor. Chem. Acc.* **2006**, *115*, 441. Basis sets available from the Dirac Web site: http://dirac.chem.sdu.dk (accessed November, 2010).
(30) DIRAC, a relativistic ab initio electronic structure program, release DIRAC10 (2010), written by Saue, T.; Visscher, L.; Jensen, H. J. Aa. with contributions from Bast, R.; Dyall, K. G.; Ekström, U.; Eliav, E.; Enevoldsen, T.; Fleig, T.; Gomes, A. S. P.; Henriksson, J.; Iliaš, M.; Jacob, Ch. R.; Knecht, S.; Nataraj, H. S.; Norman, P.; Olsen, J.; Pernpointner, M.; Ruud, K.; Schimmelpfennig, B.; Sikkema, J.; Thorvaldsen, A.; Thyssen, J.; Villaume, S.; Yamamoto, S. See http://dirac.chem.vu.nl (accessed November, 2010).
(31) DALTON, a molecular electronic structure program, Release 2.0 (2005). See http://www.kjemi.uio.no/software/dalton/dalton.html (accessed November, 2010).
(32) *CRC Handbook of Chemistry and Physics*, 82nd ed.; CRC Press: Boca Raton, FL, 2002; p 6−45.
(33) Becke, A. D. *Phys. Rev. A.* **1988**, *38*, 3098.
(34) Lee, C.; Yang, W.; Parr, R. G. *Phys. Rev. B.* **1988**, *37*, 785.
(35) Becke, A. D. *J. Chem. Phys.* **1993**, *98*, 5648.
(36) Stephens, P.; Devlin, F.; Chabalowski, C.; Frisch, M. J. *J. Phys. Chem.* **1994**, *98*, 11623.
(37) Becke, A. D. *J. Chem. Phys.* **1993**, *98*, 1372.
(38) Visscher, L.; Enevoldsen, T.; Saue, T.; Jensen, H. J. Aa.; Oddershede, J. *J. Comput. Chem.* **1999**, *20*, 1262.
(39) Hettema, H.; Jensen, H. J. Aa.; Jørgensen, P.; Olsen, J. *J. Chem. Phys.* **1992**, *97*, 1174.
(40) Salek, P.; Vahtras, O.; Helgaker, T.; Ågren, H. *J. Chem. Phys.* **2002**, *117*, 9630.
(41) Hättig, C.; Christiansen, O.; Koch, H.; Jørgensen, P. *Chem. Phys. Lett.* **1997**, *269*, 428.
(42) Norman, P.; Jensen, H. J. Aa. *J. Chem. Phys.* **2004**, *121*, 6145.
(43) Henriksson, J.; Saue, T.; Norman, P. *J. Chem. Phys.* **2008**, *128*, 024105.

(44) Dyall, K. G. *Theor. Chem. Acc.* **1998**, *99*, 366. Addendum *Theor. Chem. Acc.* **2002**, *108*, 365. Revision *Theor. Chem. Acc.* **2006**, *115*, 441. Basis sets available from the Dirac Web site: http://dirac.chem.sdu.dk (accessed Nov. 2011).
(45) Dyall, K. G. *Theor. Chem. Acc.* **2002**, *108*, 335. Erratum *Theor. Chem. Acc.* **2003**, *109*, 284. Revision *Theor. Chem. Acc.* **2006**, *115*, 441. Basis sets available from the Dirac Web site: http://dirac.chem.sdu.dk (accessed Nov. 2011).
(46) Bast, R.; Saue, T.; Henriksson, J.; Norman, P. *J. Chem. Phys.* **2009**, *130*, 024109.
(47) Ekström, U.; Norman, P.; Rizzo, A. *J. Chem. Phys.* **2005**, *122*, 074321.
(48) Ingersoll, L. R.; Liebenberg, D. H. *J. Opt. Soc. Am.* **1956**, *46*, 538.
(49) Aziz, R. A.; Slaman, M. J. *Mol. Phys.* **1986**, *57*, 825.